A lithospheric profile across northern Taiwan: from arc-continent collision to extension

Harm J.A. Van Avendonk,[1] Kirk D. McIntosh,[1] Hao Kuo-Chen,[2] Luc L. Lavier,[1] David A. Okaya,[3] Francis T. Wu,[3,4] Chien-Ying Wang,[2] Chao-Shing Lee[5] and Char-Shine Liu[6]

[1] *Institute for Geophysics, Jackson School of Geosciences, University of Texas at Austin, Austin, TX, USA. E-mail:* harm@ig.utexas.edu
[2] *Institute of Geophysics, National Central University, Jhongli, Taiwan*
[3] *Department of Earth Sciences, University of Southern California, Los Angeles, CA, USA*
[4] *Department of Geological and Environmental Sciences, State University of New York at Binghamton, Binghamton, NY, USA*
[5] *Department of Geophysics, National Taiwan Ocean University, Keelung, Taiwan*
[6] *Institute of Oceanography, National Taiwan University, Taipei, Taiwan*

SUMMARY

During arc-continent collision, buoyant sections of sediments and rifted continental crust from a subducting plate will accrete to the forearc of the upper plate as long as this backstop remains intact. Deformation of the oceanic arc and forearc block may ultimately lead to accretion of these mafic rock units to the new orogen. The Taiwan mountain belt, which formed at ∼6.5 Ma by oblique convergence between the Eurasian passive margin and the overriding Luzon arc in northern Taiwan, offers important insight in this process, since the collision is more advanced in the north than in the south. The incipient stage of arc-collision can be studied in southern Taiwan, while the northern portion of the orogen is presently undergoing collapse due to a flip in the subduction polarity between the Eurasian Plate and the Philippine Sea Plate. In this study, we seismically image the structure of the northern section of the mountain belt with a tomographic inversion. We present marine and land-based seismic refraction data, as well as local earthquake data, from transect T6 of the Taiwan Integrated Geodynamic Research (TAIGER) program across the Taiwan mountain belt and the adjacent Ryukyu arc. Our 2-D compressional seismic velocity model for this transect, which is based on a tomographic inversion of 10 213 *P*-wave arrival times, shows that the Eurasian crystalline continental crust thickens from ∼24 km in the Taiwan Strait to ∼40 km beneath the eastern Central Range of Taiwan. The detailed seismic velocity structure of the Taiwan mountain belt shows vertical continuity in the upper 15 km, which suggests that rocks are exhumed to the surface here from the middle crust in a near-vertical path. The continental crust of the westernmost Ryukyu arc is almost as thick (∼40 km) as in the adjacent northern Central Range of Taiwan, and it appears to override the leading edge of the Philippine Sea Plate offshore northeastern Taiwan. If we assume that the western Ryukyu arc crust also thickened in the collision, then the mountain belt is wider and less thick in northern Taiwan than in central Taiwan (∼50 km), which may be the result of post-collisional extension in the north.

Key words: Seismic tomography; Continental margins: convergent; Crustal structure.

1 INTRODUCTION

Where passive continental margin crust enters a trench and collides with the overriding forearc and island arc, lateral compression will lead to intense shortening and uplift in the incoming plate until the forearc can no longer form a backstop to the growing crustal wedge (Brown *et al.* 2011). Mechanical failure of the arc/forearc block can lead to a reversal of the polarity of subduction (Draut &

Clift 2013), the release of compressive stresses, and collapse of the young orogen (Dewey 1988; Rey *et al.* 2001). Modern examples of arc-continent collision can be found in the Banda Sea (Bowin *et al.* 1980; Audley-Charles 2004), in Taiwan (Teng 1990; Byrne *et al.* 2011), between Venezuela and the southern Caribbean arc (Avé Lallemant 1997; Kroehler *et al.* 2011), between northern Papua New Guinea and the New Britain arc (Cooper & Taylor 1987; Abers & Roecker 1991), and in Kamchatka (Geist & Scholl 1994;
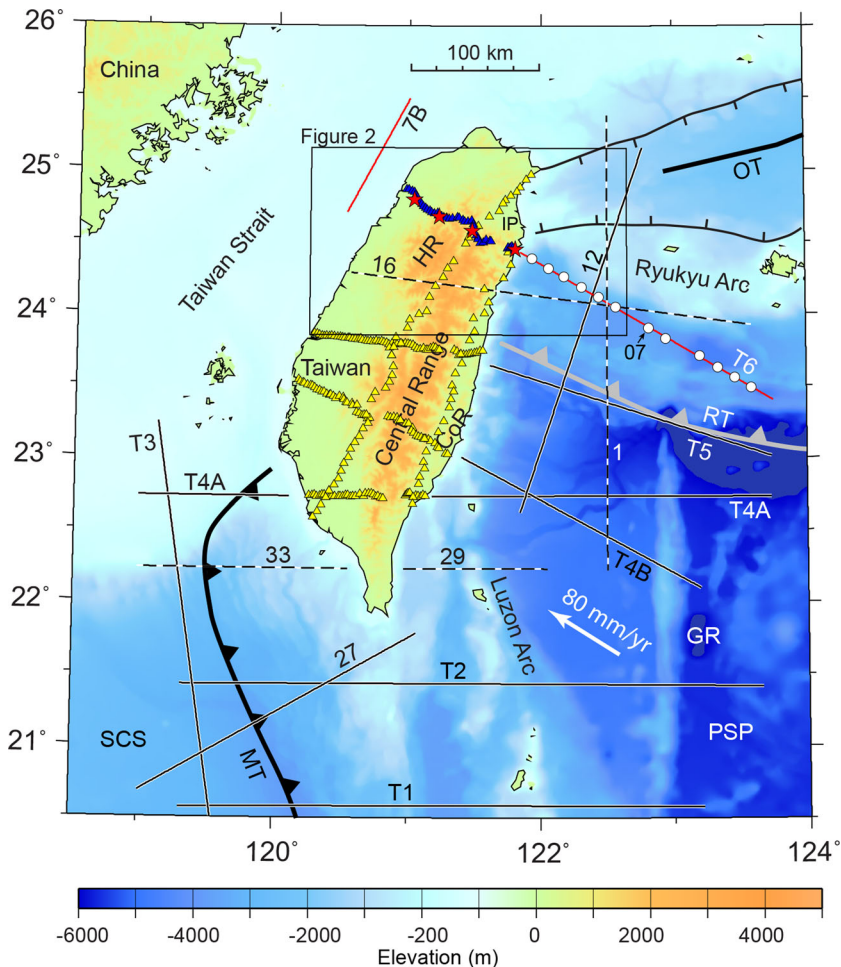
Figure 1. Elevation map of Taiwan and adjacent areas with major tectonic features, overlain by regional seismic transects. CoR, Coastal Range; GR, Gagua Ridge; HR, Hsüehshan Range; IP, Ilan Plain; MT, Manila Trench; OT, Okinawa Trough; PSP, Philippine Sea Plate; RT, Ryukyu Trench; SCS, South China Sea. Plate velocity of PSP relative to Eurasia (white arrow) is from Hsu *et al.* (2009). Black/white dashed lines are seismic transects from the TAICRUST project (Wang *et al.* 2001; McIntosh *et al.* 2005). All other transects (either black or red) were gathered during the TAIGER project. Yellow and blue triangles show the location of land seismic instruments; white circles the ocean-bottom seismometer (OBSs) on transect T6.

Konstantinovskaya 2011). One of the major challenges in studies of arc-continent collision is to understand the temporal evolution of these complex plate boundaries.

Continental collision and post-orogenic extension are currently both in progress in different parts of the Taiwan mountain belt (Teng 1996). In central Taiwan, convergence between the Eurasian and Philippine Sea plates (Yu & Kuo 2001) is deforming the continental crust of the Chinese margin into a thick wedge that is compressed against the northern Luzon arc (Brown *et al.* 2012; Fig. 1). Here the Central Range and Hsüehshan Range are experiencing rapid uplift and exhumation (Fuller *et al.* 2006; Simoes *et al.* 2007), but the north end of the Taiwan mountain belt is currently extending and subsiding (Ching *et al.* 2011b). The extension and collapse of the orogen are caused by the southwestward propagation of the Okinawa trough into northeastern Taiwan (Suppe 1984; Sibuet *et al.* 1998; Clift *et al.* 2008; Huang *et al.* 2012). Receiver function analyses (Kim *et al.* 2004) and regional seismic velocity models (Kuo-Chen *et al.* 2012a) show that the crust of Central Taiwan is much thicker (50 km) than to the north (33 km), but more detailed seismic images are needed to characterize how the mountain belt is thinning at the intersection with the Ryukyu subduction system.

In 2008 and 2009, U.S. and Taiwanese scientists acquired several long-offset 2-D seismic transects across the convergent margin

between the Eurasian and Philippine Sea plates in the Taiwan Integrated Geodynamic Research (TAIGER) project (Klingelhoefer *et al.* 2012; Lester *et al.* 2013; McIntosh *et al.* 2013; Eakin *et al.* 2014; Van Avendonk *et al.* 2014). Due to the oblique angle between the plate boundary and the overriding Luzon arc (Suppe 1981), the TAIGER transects imaged a more mature stage of the arc-continent collision in the north than in the south. In this paper, we present a seismic velocity model based on an analysis of active-source and local earthquake data for TAIGER Transect 6 across northern Taiwan and the adjacent forearc of the Ryukyu subduction system. The dense data coverage along this northernmost TAIGER transect shows structural details in the mountain belt that provide new insight in the formation and subsequent extensional collapse of this well-studied mountain belt.

2 TECTONIC SETTING

The Taiwan orogen developed ∼6.5 Ma in northern Taiwan (Lin *et al.* 2003) when convergence between the Philippine Sea Plate and Eurasian Plate closed up the northern South China Sea. According to McIntosh *et al.* (2013), the accretion of blocks of the Chinese rifted margin crust to the west-facing prism of the
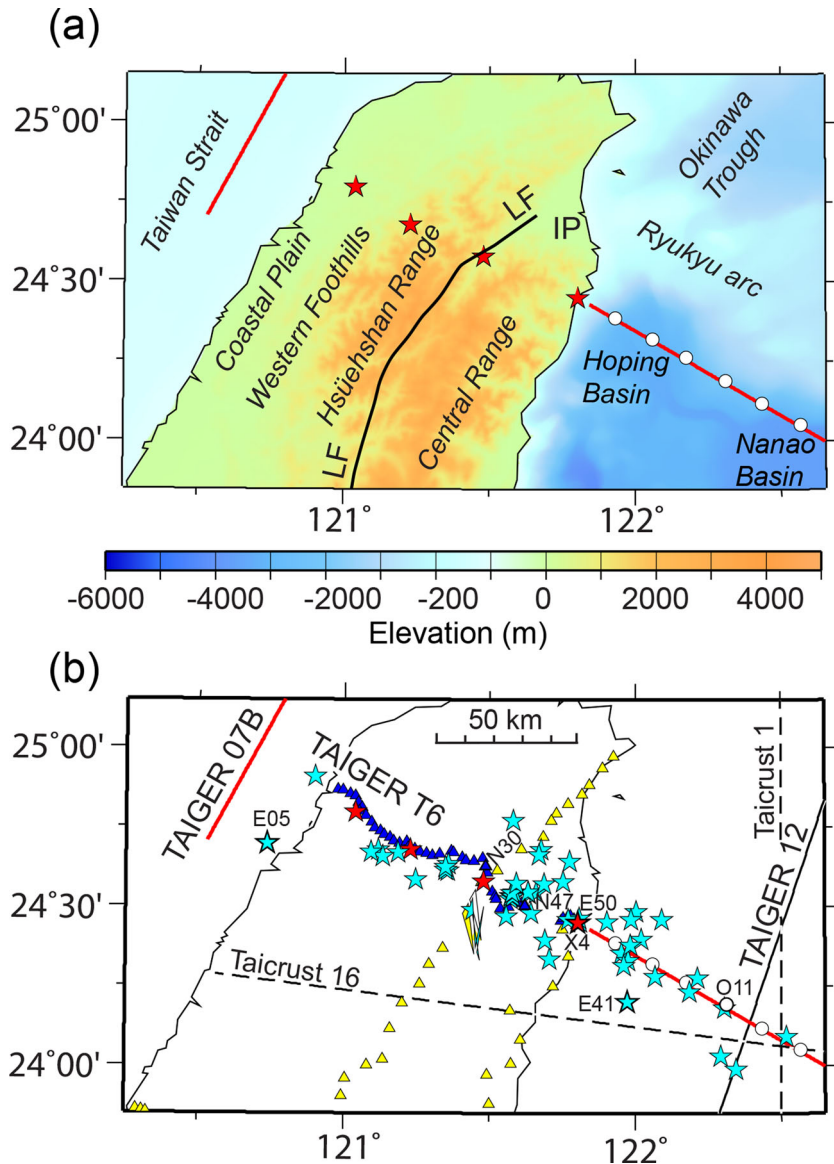
Figure 2. Maps of northern Taiwan and transect T6. (a) Topography and major tectonic features. IP, Ilan Plain; LF, Lishan Fault. Land explosive shots (red stars) and OBSs (white circles) illustrate data coverage on transect T6. Marine shot lines used for this study shown as red lines. (b) TAIGER (solid red) and TAICRUST (dashed black) lines offshore northern Taiwan, shown with T6 explosive shots and land seismometer, and local earthquakes (cyan stars) used in the tomography analysis. Data records from labelled earthquakes, explosive shots, land stations and OBS are shown in Figs 4–7.

Luzon arc initiated the growth of the Central Range. Over the course of a few million years the collision propagated southward (Liu *et al.* 2001; Lee *et al.* 2006), and in central and northern Taiwan the material flux in the orogen subsequently reached a steady state (Willett & Brandon 2002; Simoes & Avouac 2006). In this mature portion of the arc-continent collision, five north–south trending tectonic domains can be recognized in the mountain belt (Ho 1986; Huang *et al.* 2006): (1) A foreland basin in the coastal plain in the west, (2) a fold-thrust belt in the Western Foothills, (3) an inverted Palaeogene sedimentary basin from the South China Sea passive margin in the Hsüehshan Range, separated by the Lishan Fault from (4) the Central Range, where metamorphic continental basement is exposed and (5) fragments of Luzon arc basement and intra-arc basins in the Coastal Range in the east (Fig. 2). In central Taiwan, the orogen is accommodating 80 mm yr^{-1} of NW–SE convergence at present (Hsu *et al.* 2009; Huang *et al.* 2010).

Shallow sediments of the foreland basin along the west coast of Taiwan are accreted in the fold-thrust belt, whereas deeper foreland deposits underthrust the Western Foothills along a shallow detachment without significant deformation (Suppe 1981; Yue *et al.* 2005). However, there is an increasing volume of geological and geophysical evidence that these deeper strata and crystalline basement are engaged in mountain building as well (Mouthereau & Lacombe 2006; Bertrand *et al.* 2009; Brown *et al.* 2012; Kuo-Chen *et al.* 2012a; Van Avendonk *et al.* 2014). Cooling ages of exhumed rocks from the Eurasian passive margin indicate that deep sediment underplating has driven the Neogene uplift in the Taiwan mountain belt. The Hsüehshan Range and Central Range record strong uplift and exhumation in the last 1 Myr (Lee *et al.* 2006; Simoes *et al.* 2007), due to the increasing compression between thick continental crust of the Taiwan Strait and the Luzon arc. In northeastern Taiwan the Coastal Range disappears just north of the intersection with the Ryukyu trench, so the Luzon arc appears to subduct with
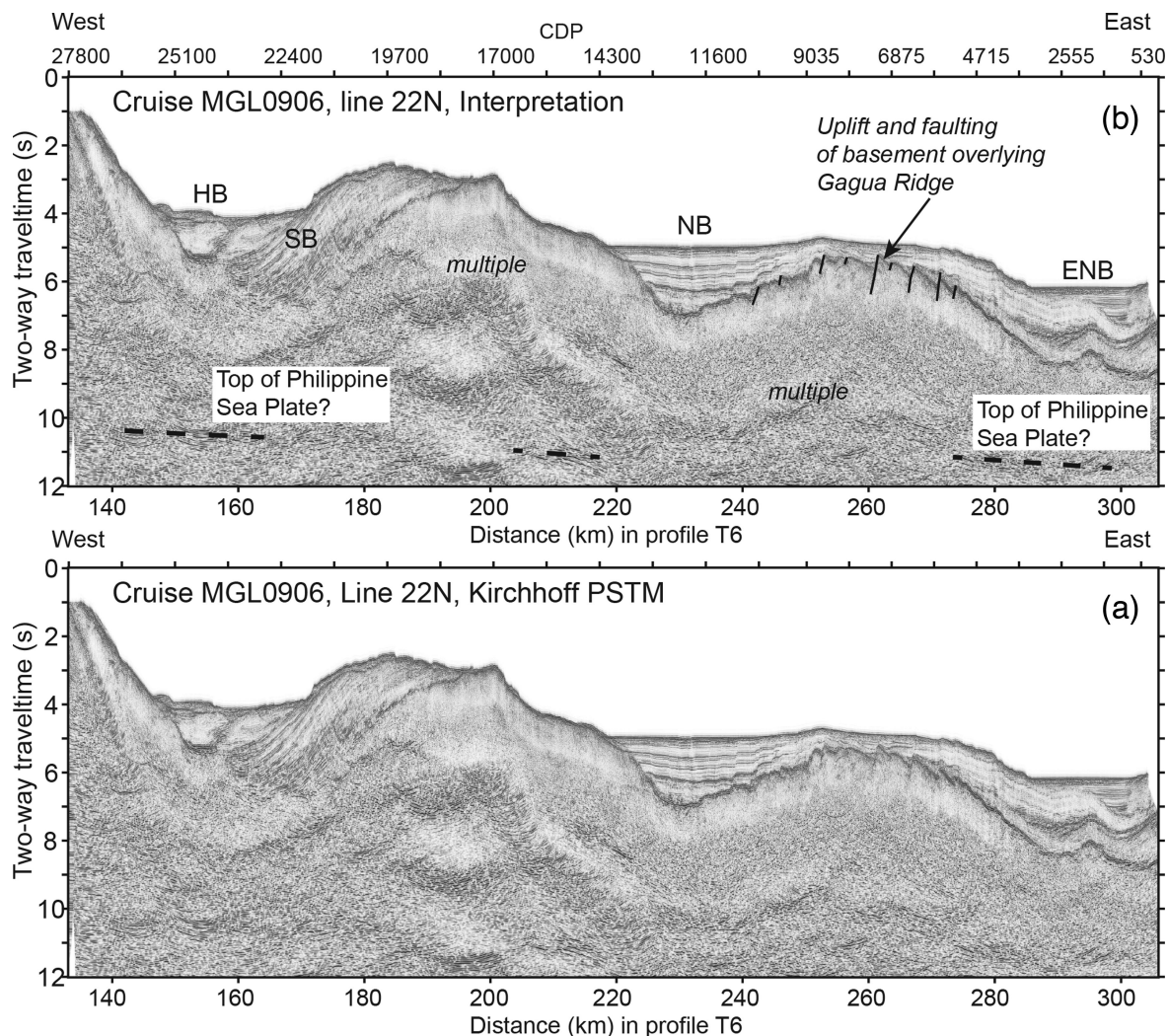
Figure 3. (a) Time-migration of marine seismic reflection data from TAIGER transect T6 east of Taiwan. (b) Interpretation of the seismic reflection data. HB, Hoping Basin; NB, Nanao Basin; SB, Suao Basin; ENB, Eastern Nanao Basin. Dashed black lines show weak reflections interpreted as top of Philippine Sea Plate beneath the Ryukyu forearc crust and prism.

the Philippine Sea Plate beneath the Ryukyu arc (Fig. 1). As a result of this subduction polarity flip in the convergence between the Eurasian Plate and Philippine Sea Plate, uplift of the Central Range is waning in northern Taiwan (Huang *et al.* 2012).

The east–west trending western portion of the Ryukyu subduction system consists from north to south of (1) the Okinawa Trough, (2) the nonvolcanic Ryukyu arc, (3) a forearc that includes the Hoping and Nanao basins, (4) an accretionary wedge and (5) incoming oceanic crust and sediments from the Philippine Sea Plate (Sibuet *et al.* 1998; Lallemand *et al.* 1999; Klingelhoefer *et al.* 2012). This segment of the Ryukyu arc is advancing southward over the Philippine Sea Plate with a velocity of 73 mm yr^{-1} relative to the stable Eurasian Plate (Nakamura 2004), while the Okinawa Trough backarc basin opens rapidly to the north, leading to extension in the Ilan Plain of northeastern Taiwan. Since the Manila trench and Ryukyu trench subduction systems meet at right angles in northeastern Taiwan, the two deep slabs must interact at depth, which can explain the large amount of local seismicity and surface deformation in this area (Wu *et al.* 2009; Lallemand *et al.* 2013). As the Philippine Sea Plate dives beneath the Ryukyu arc northeast of Taiwan, it continues to act as a 'subducted indentor', pressing against the lower lithosphere of the Eurasian Plate in an oblique direction

(Wu *et al.* 2009). The continental crust overriding this transpressive plate boundary is currently in extension (Hou *et al.* 2009).

3 TAIGER SEISMIC DATA

3.1 Experiments

The TAIGER experiment was a U.S.–Taiwanese collaborative project to image the Taiwan mountain belt and surrounding areas on a lithospheric scale. Besides the acquisition of long-period magnetotelluric data (Bertrand *et al.* 2009, 2012), a large effort was made to gather land-based and marine seismic data (McIntosh *et al.* 2013; Van Avendonk *et al.* 2014; Wu *et al.* 2014). In this paper, we present the data from TAIGER transect T6, which lies across northern Taiwan between the Taiwan Strait and the Ryukyu accretionary wedge.

In 2008 we conducted an on-land explosion seismic experiment in Taiwan to constrain the crustal structure of the mountain belt. Explosive shots were recorded on linear arrays of vertical component seismic stations that were spaced 200 m apart. In 2009 we used the R/V *Marcus Langseth* to image offshore areas around Taiwan.
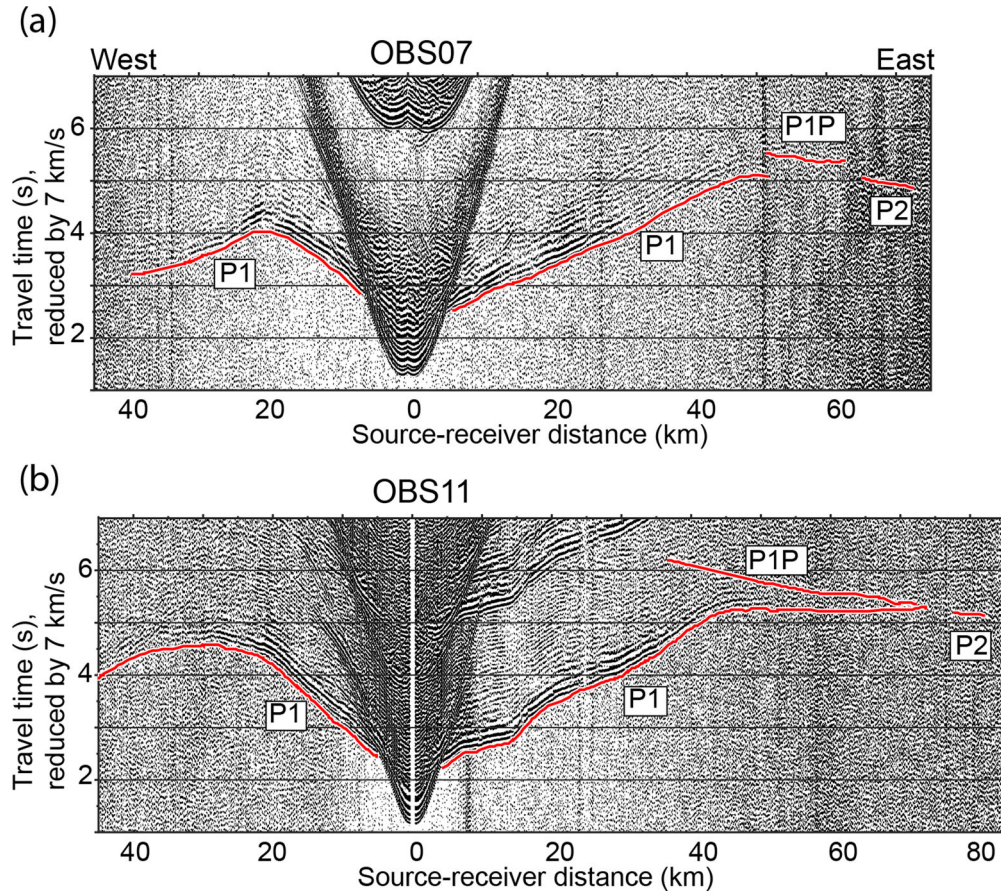
Figure 4. Wide-angle seismic data from OBS 11 and OBS 07 on transect T6, east of Taiwan. The solid red lines outline the traveltime picks of wide-angle phases used in this study. *P1*, crustal seismic refraction; *P1P*, reflection from the base of Eurasian crust; *P2*, deeper refraction.

The *Langseth* traversed the main TAIGER transects twice with its 6600 in^3 source array to optimize the quality of seismic reflection and refraction data. Shots spaced 50 m apart were recorded for 15 s by the *Langseth*'s 6-km-long streamer for MCS imaging.

TAIGER transect T6 is oriented oblique to the Ryukyu trench east of Taiwan (Fig. 1). Consequently, the MCS line that was shot here by the R/V *Marcus Langseth* traverses the Hoping and Nanao forearc basins in the northwest, and its southeast end point lies on the Ryukyu accretionary prism 35 km north of the trench (Fig. 3). From several Taiwanese vessels we deployed four-component OBSs at 15 km spacing along these seismic lines to collect wide-angle data, using a shot interval of 150 m to minimize previous shot noise. For the duration of the marine seismic experiment, arrays of 2 Hz land seismometers recorded both the offshore air-gun shots and local earthquakes.

3.2 Seismic phases

Twelve ocean-bottom seismometers from National Taiwan Ocean University (NTOU) recorded seismic refractions from the *Langseth* air-gun shots east of Taiwan (Figs 1 and 2). To 40 km source–receiver offset we mostly observe waves turning in the Ryukyu forearc crust and prism (*P1* in Fig. 4). However, at approximately 50 km or larger source–receiver offsets, a deep wide-angle seismic reflection (*P1P* in Fig. 4), appears in some of the OBS record sections. As we discuss in the next section, this *P1P* phase may be a wide-angle reflection from the base of the Eurasian crust. Over a limited range of larger source–receiver offsets (70–100 km) we

identify a phase (*P2*) that must turn at a depth larger than that of the *P1P* reflection. Due to the shallow water and permitting restrictions we did not gather MCS or OBS seismic refraction data in the Taiwan Strait along line T6.

An array of 45 land-seismic stations from IRIS/PASSCAL (the Program for Array Seismic Studies of the Continental Lithosphere) recorded *Langseth* air-gun shots from line T6 in the Philippine Sea, and also from marine seismic line 7B, which was oriented parallel to the coast in the Taiwan Strait. In the record sections (Fig. 5) we can recognize the same phases *P1*, *P1P* and *P2* that were observed in the OBS data, but in the onshore-offshore data we can see the *P1P* phases to source-receiver offsets as large as 150 km. *P2* phases with a high apparent velocity (>7 km s^{-1}) are observed in the onshore-offshore records at offsets more than 100 km. This suggests that the Eurasian crust is thicker on-land than offshore in the Taiwan Strait. The observation of *P1P* arrivals also makes the onshore-offshore data from line T6 significantly richer than those of TAIGER transect T5, where these phases were not identified. The wide-angle reflection *P1P* was also recognized in one of the four explosion seismic refraction shot gathers. Seismic stations on the west coast recorded this deep reflection from Shot 4 at the east coast (Fig. 6). All explosive shot records show a clear *P1* seismic refraction, and Shot 4 also registered a mid-crustal wide-angle reflection that we did not use in our analysis.

The TAIGER onshore-offshore seismic stations, which were deployed over three months during the *Langseth* program around Taiwan, also recorded a large number of local earthquakes (Kuo-Chen *et al.* 2012a). These earthquakes can provide important constraints
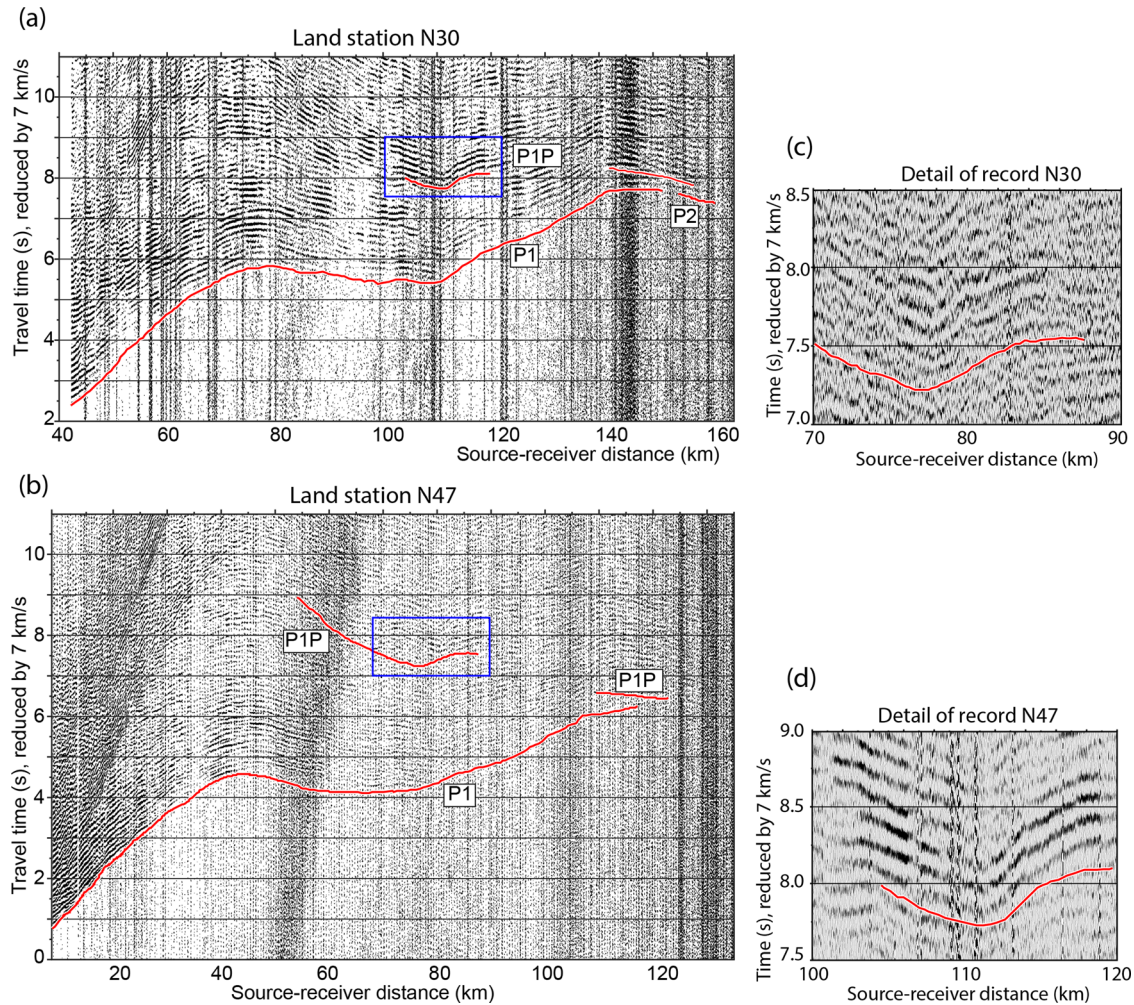
Figure 5. Wide-angle seismic data from land stations N30 (a) and N47 (b) on transect T6, recording air-gun shots east of Taiwan. The solid black lines outline the traveltime picks of wide-angle phases used in this study. Blue boxes indicate details of the data shown in (c) and (d).
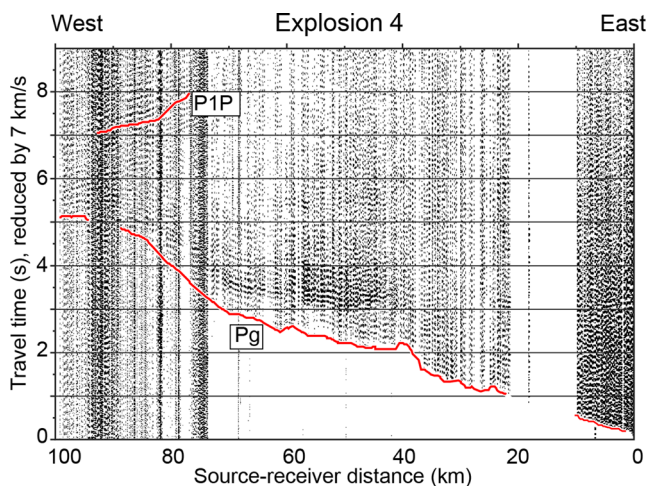

Figure 6. Wide-angle seismic refractions from explosive shot 4, near the east coast of Taiwan. The solid red lines outline the traveltime picks of wide-angle phases used in this study.

on the deep lithospheric structure along transect T6, if they occurred within 10–15 km of the vertical profile, and if their origin time and location can be determined accurately. For 52 local earthquakes with a magnitude $M_w \geq 1.5$, we determined compressional and shear wave

arrivals on a few different transects of the TAIGER seismic array. As in the case of the tomographic analysis of TAIGER transect T5 (Van Avendonk *et al.* 2014), we relocated these local earthquakes with regional *P*-wave and *S*-wave velocity models (Kuo-Chen *et al.* 2012a,b). Many of these events occurred in the Central Range or Hoping basin, but some others were relocated in western Taiwan, or farther east in the Philippine Sea (Fig. 2b). In Fig. 7 we show records of compressional and shear wave arrivals of three such local earthquakes on stations on TAIGER transect T6.

4 SEISMIC DATA ANALYSIS

4.1 Seismic reflection data processing

We stacked and migrated the marine seismic reflection data profile T6, and suppressed seafloor multiples to bring out seismic reflections from the base of the Ryukyu forearc. We used the seismic processing scheme of Lester & McIntosh (2012), which includes bandpass filtering, iterative multiple modelling and subtraction, velocity analysis, normal moveout correction, stacking and Kirchhoff time migration. The resulting image shows relatively recent, flat-lying sediments on tilted older sediments in the Hoping basin (Fig. 3), indicating that the basement 20–30 km east of Taiwan was also deformed in the recent arc-continent collision. The Nanao basin
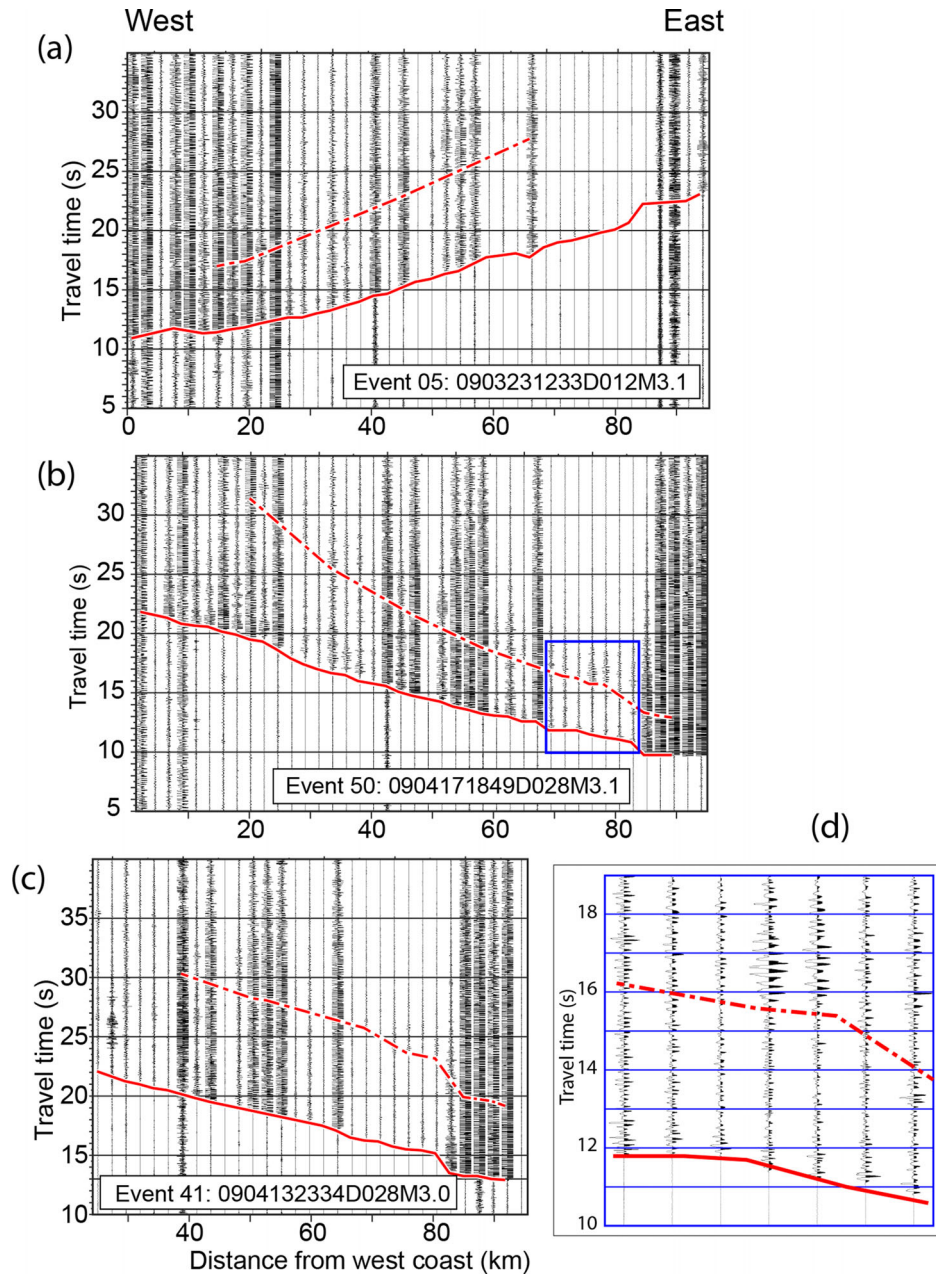
Figure 7. Local earthquakes with an epicentre near transect T6, recorded by the T6 onshore-offshore land seismic array. The epicentres of events 05 (a), 50 (b) and 41 (c) are indicated in Fig. 2(b). (d) shows an enlarged portion of the data from event 50. The solid red line outlines the traveltime picks of compressional waves, and the dashed red lines marks the arrival times of shear waves that were used for event relocation.

does not exhibit the same rotation of accumulated sediment. Farther east, the basement of the Ryukyu forearc is uplifted and faulted where the Gagua Ridge subducts beneath the Eurasian Plate. The top of the Philippine Sea Plate can be distinguished in two locations in the seismic reflection image at 10 s two-way traveltime (Fig. 3).

4.2 Traveltime tomography

4.2.1 Ray tracing and inversion

The combined onshore–offshore seismic refraction data set for TAIGER transect T6 provides dense coverage of sources and receivers across the western and eastern shoreline of northern Taiwan, which we use to obtain a 2-D crustal seismic velocity model.

Table 1. The number of picks for each data type used in the tomographic inversion of the TAIGER T6 study. In the earthquake records we did not distinguish between *P1* and *P2* phases.

	P1	*P2*	*PmP*	Total
OBS	3718	50	422	4190
Sea-land	2628	44	907	3579
Explosion	1258	0	47	1305
Earthquake	1139 (P1 and P2)		0	1139
.				

For each of the data types, we bandpass filtered the record sections before picking the arrival times. We gathered a total of 10 213 traveltime picks for the *P1, P1P* and *P2* arrivals in the T6 data set (Table 1). Uncertainties between 50 and 250 ms were assigned to these

traveltime picks based on the signal-to-noise ration and quality of the observations.

To invert the T6 traveltime data set for seismic velocity structure we adopted the iterative tomography method of Van Avendonk *et al.* (2004), which was previously used to construct a seismic velocity model for TAIGER transect T5 in central Taiwan (Van Avendonk *et al.* 2014). We first defined a preliminary seismic velocity model for Taiwan and the Ryukyu arc based on prior work (McIntosh *et al.* 2005; Kuo-Chen *et al.* 2012a; Theunissen *et al.* 2012). Though the choice of the starting model can affect the convergence speed of the iterative inversion, the final seismic velocity image should not depend on the starting model if the regularization in each linear inversion step does not bias the solution to the starting model (Hole 1992; Toomey *et al.* 1994). The smoothness and flatness constraints employed in our method (Van Avendonk et al. 2004) act on the resulting velocity model, not on the model perturbation, to minimize the effect of the starting model.

We traced rays for the observed refractions (*P1*, *P2*) and wide-angle reflections (*P1P*) in this starting model for profile T6 with the shortest path method (Moser 1991) and ray bending (Moser *et al.* 1992; Van Avendonk *et al.* 2001). For the local earthquakes we used 3-D ray tracing to obtain the correct geometry and traveltimes. In addition, unlike in the active-source seismic data of transect T6, we were not able to distinguish between *P1* and *P2* phases in the earthquake records, so we ray traced these arrivals as first-arriving phases. We iterated between ray tracing and 2-D regularized inversions for seismic velocity structure and Moho depth (Van Avendonk *et al.* 2004) until the traveltime misfit was reduced to 145 ms, with a normalized χ^2 of 1.0. The misfit of the earthquake arrivals (280 ms) were relatively large, which is consistent with the larger uncertainty in these traveltime picks.

We examine the ray paths and data fit for different data types after the inversion of transect T6 traveltimes. The ray paths for the four on-land explosions across northern Taiwan mostly sample the upper 5 km, but the *P1P* phase in our record of Shot 4 is consistent with a reflection from a depth of more than 30 km beneath the Western Foothills (Fig. 8a). The crust of the Ryukyu forearc is reasonably well covered by ray paths from seismic refractions in the OBS data (Fig. 8b), but we obtain little insight in what lies beneath the Ryukyu crust, because relatively few *P2* arrivals were observed in the marine seismic refraction data. The onshore-offshore data across the east coast of Taiwan show good coverage of the deep crust with *P1P* and *P2* arrivals (Fig. 8c). The onshore recording of line 7B in the Taiwan Strait gave us similar constraints on the west side of Taiwan (Fig. 1), but this data set was smaller since only one of the Langseth air-gun shots here lies directly on transect T6. Last the local earthquake data greatly complement the ray coverage of the active-source data at larger depth, though the uncertainty and misfits for earthquake traveltimes are larger (Fig. 8d).

4.2.2 *Model resolution*

The seismic velocity profile of TAIGER transect T6 gives a view of the crust of the northern Taiwan Strait, the northern Taiwan Mountain belt, and the adjacent Ryukyu forearc and prism (Fig. 9). With the help of local earthquake recordings we were able to infer seismic velocity structure to a depth of 70 km in the mantle beneath Taiwan along transect T6. Earthquakes also helped to improve our seismic velocity image of the mountain belt. Although the methodology that we used here closely followed the analysis of TAIGER transect T5 to the south (Van Avendonk *et al.* 2014), we were able

to include *P1P* reflections from the base of the Eurasian crust in the tomographic inversion, which allowed us to resolve this boundary. Since these wide-angle reflections were only sporadically observed in the T5 data set, Van Avendonk *et al.* (2014) produced a seismic velocity image for that profile that was based only on first-arriving phases.

We derive an estimate of model resolution from the generalized inverse that produced our final seismic velocity model (Van Avendonk *et al.* 2004). In Fig. 10 we show how the ray path geometry in our tomographic inversion can constrain model features of two different sizes. Resolution values greater than 0.5 can be considered adequately resolved (Van Avendonk *et al.* 2004). The resolution tests indicate that seismic structure with a lateral size of 16 km can be resolved in the upper crust, but not in the lower crust. Model features that span 32 km have sufficient resolution in the entire crust and even in parts of the underlying mantle. The Moho is well resolved in the eastern and western flank of the orogen. Straight beneath the Central Range and beneath much of the Ryukyu forearc the base of the Eurasian crust is not well resolved.

5 RESULTS

We here describe the 2-D seismic velocity model for transect T6 that we obtained from the tomographic inversion. The seismic line lies entirely on crust of the Eurasian Plate (Fig. 1), but near the east coast of Taiwan it crosses a major left-lateral shear zone. The shear zone, which is illuminated by frequent seismicity at 135 km in our model (Fig. 9) separates the Taiwan mountain belt from the Ryukyu arc/forearc block (Fig. 1).

5.1 Taiwan mountain belt

On transect T6 the seismic velocity structure of the pre-collision crust in the Taiwan Strait is illuminated only by the onshore recording of air-gun shots from line 7B (Fig. 1). Though the resolution of seismic structure at the far northwest end of our profile is not good (Fig. 10), we think that a thickness of 28 km for the undeformed Chinese margin crust and sediments, with seismic velocity increasing from 4.0 km s^{-1} at the seafloor to 7.0 km s^{-1} at the Moho, is a plausible result (Fig. 9). If the 5.0 km s^{-1} velocity contour lies approximately at the depth of pre-Miocene basement (Camanni *et al.* 2014; Van Avendonk *et al.* 2014) then the sediment cover on the incoming Eurasian basement at the west end of our profile may be 4–5 km (Fig. 9), which is consistent with existing marine seismic reflection data (Lacombe *et al.* 2003). Towards the west coast of Taiwan the basement depth increases to roughly 10 km. The asymmetric shape of this basement low, with a steeper eastern slope beneath the Western Foothills, is typical for the foredeep of the Taiwan mountain belt (Chou & Yu 2002; Simoes & Avouac 2006).

Our model shows distinct seismic velocity anomalies in the upper crust of northern Taiwan that correspond with the major tectonic units of the mountain belt (Fig. 9). The seismic velocity in the Hsüehshan Range increases rapidly with depth from ~5.0 km s^{-1} to more than 5.5 km s^{-1} in the first few kilometres. At 100 km distance in our model, the Lishan fault is characterized by *Vp* lower than 4.5 km s^{-1}. Farther east, the Central Range has seismic velocities higher than 6 km s^{-1} in the upper crust. In contrast, the middle crust of northern Taiwan appears more homogeneous with a seismic velocity between 5.5 and 6.0 km s^{-1}, but the smoothed seismic velocity inversion may not represent fine structure at this depth
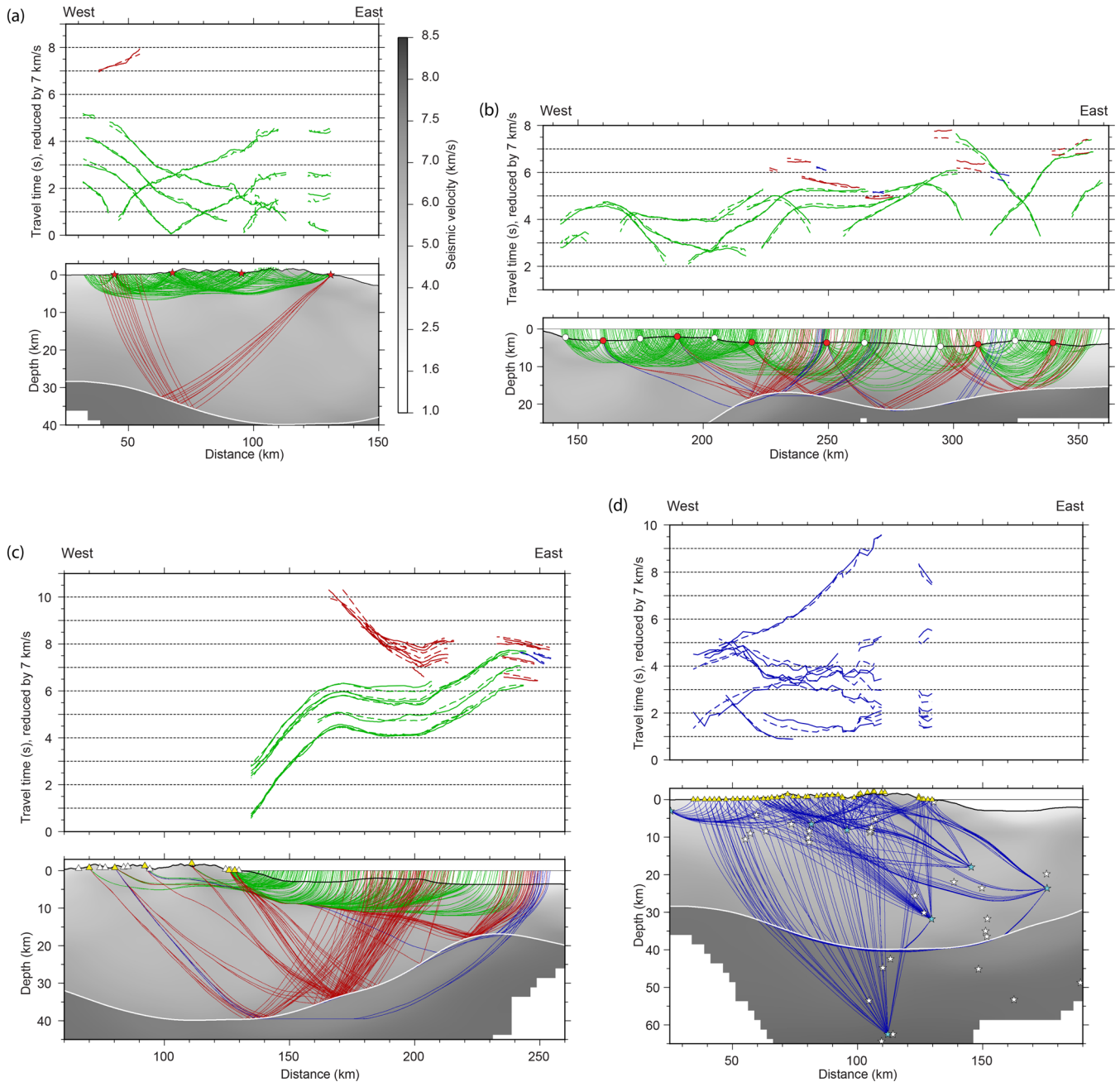
Figure 8. (a) Bottom: ray paths calculated in the new seismic velocity model for the four explosive shots (red stars) on transect T6. Crustal refractions *P1* are shown in green, and reflections *P1P* in red. White line represents the Eurasian Moho. Top: picked (solid) and calculated (dashed) traveltimes for all wide-angle refractions and reflections in the explosion seismic data. (b) Bottom: ray paths calculated in the new seismic velocity model for selected OBSs (red circles) on transect T6. Crustal refractions *P1* are shown in green, wide-angle reflections *P1P* in red, deeper *P2* refractions in blue. Top: picked (solid) and calculated (dashed) traveltimes for selected wide-angle refractions in the OBS seismic data. (c) Bottom: ray paths calculated in the new seismic velocity model for selected land seismic stations (yellow triangles) and air-gun shots on the eastern portion of transect T6. Refractions *P1* are shown in green, wide-angle reflections *P1P* in red, *P2* refractions in blue. Top: picked (solid) and calculated (dashed) traveltimes for selected wide-angle refractions in the onshore-offshore seismic data. (d) Bottom: ray paths (in blue) projected on the vertical plane through the new seismic velocity model for selected land earthquakes (light blue stars) recorded by onshore-offshore stations (yellow triangles) on transect T6. Top: picked (solid blue) and calculated (dashed blue) traveltimes for selected earthquake compressional wave arrival times.

because the resolution is lower here (Fig. 10). On the other hand, it appears that the seismic velocity in the upper crust of the Hsüehshan Range and Central Range is not lower than the average *Vp* of the middle crust.

The Moho beneath northern Taiwan forms a wide crustal root, increasing in depth from 28 km beneath the west coast to a maximum

of 38 km just west of the strike-slip zone along the east coast (Fig. 9). The seismic velocity in the lower crust of Taiwan is 6.0–6.5 km s^{-1}, which is lower than in the lower crust of the adjacent Taiwan Strait. In our seismic velocity model, the mantle beneath Taiwan increases with depth from just below 8.0 km s^{-1} at the Moho to more than 8.0 km s^{-1} at 70 km depth. Since the deeper mantle lithosphere is
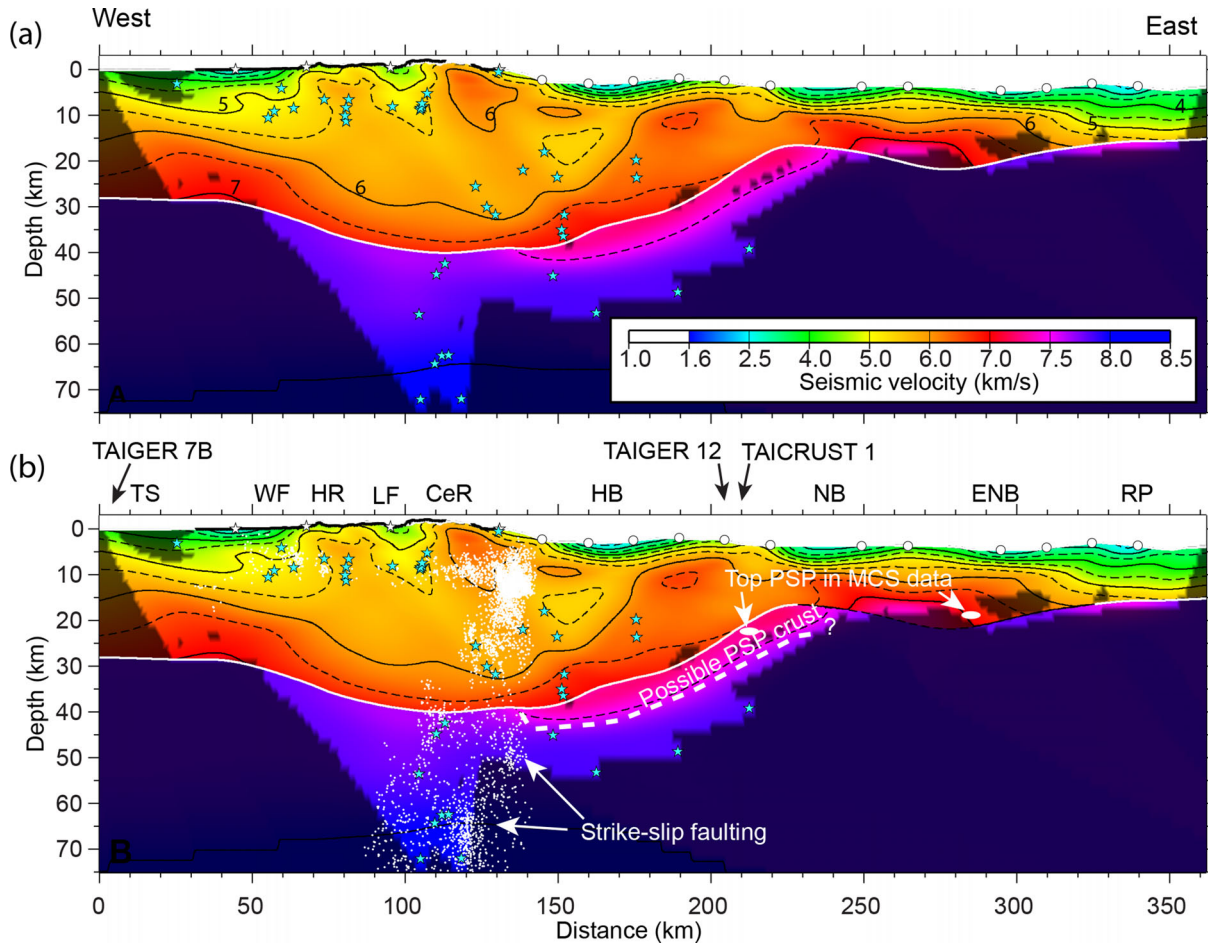
Figure 9. (a) Seismic velocity model for transect T6 based on a tomographic inversion of the TAIGER active-source and local earthquake arrival times. Seismic velocities are contoured at 1.0 km s^{-1} (solid) and 0.5 km s^{-1} (dashed) intervals. White solid line marks the model boundary constrained by *P1P* reflections, mostly following the Moho of Eurasian crust. Light blue stars mark the projected location of local earthquakes used in the inversion. Explosive shots (white stars), OBS (white circles) and land seismic stations (thick black line on surface 30 and 130 km) illustrate the source–receiver geometry. Portions of the seismic velocity model without ray coverage are shaded. (b) Seismicity between 2000 and 2009 within 15 km of transect T6 is marked on seismic velocity model with white dots. White dashed line: Interpreted outline of Philippine Sea Plate crust beneath Eurasian crust of the Ryukyu arc. TS, Taiwan Strait; WF, Western Foothills; HR, Hsüehshan Range; LF, Lishan Fault; CeR, Central Range; HB, Hoping Basin; NB, Nanao Basin; ENB, Eastern Nanao Basin; RP, Ryukyu Prism.

only covered by the near-vertical ray paths from local earthquakes (Fig. 8d), we do not have the necessary depth resolution to interpret its seismic velocity.

5.2 Ryukyu forearc and prism

Between 135 and 360 km (Fig. 9) the velocity profile for line T6 obliquely crosses the Ryukyu arc/forearc block and accretionary prism. The Eurasian Moho beneath the Hoping Basin varies in depth from 38 km in the northwest to 25 km in the southeast. The crust thins to just ∼12 km beneath the Nanao Basin, though some sections of the southeastern portion of the T6 velocity profile are not well constrained. The Ryukyu arc crust between the Hoping Basin (at 170 km in Fig. 9) and the Eastern Nanao Basin (300 km) has a seismic velocity mostly >6.0 km s^{-1}, but to the southeast the seismic velocities rapidly drop to 3–5 km s^{-1}. Klingelhoefer *et al.* (2012) interpreted this transition as the boundary between the Ryukyu forearc basement and the prism.

Between the east coast of Taiwan (135 km) and the Nanao Basin (230 km) our tomographic model shows a 5–10 km thick layer beneath the Ryukyu Moho where the seismic velocity is as low

as 7.0 km s^{-1} (Fig. 9). These relatively low seismic velocities are constrained mostly by the onshore-offshore data (Figs 5 and 8c). At larger depth we observe normal mantle seismic velocities (>8.0 km s^{-1}) that we would expect for the mantle of the Philippine Sea Plate. This zone with 7.0 km s^{-1} seismic velocities could therefore be Philippine Sea Plate ocean crust, or Luzon arc crust, that is underthrusting the Ryukyu arc to the north. This interpretation is consistent with the sparse observations of the top of basement of the Philippine Sea Plate in the MCS image of transect T6 (Fig. 3). Unfortunately, the OBS wide-angle seismic refraction data do not constrain the position of the subducting Philippine Sea Plate ocean crust here or farther to the southeast, because we did not record enough long-offset seismic refractions that turned beneath the Ryukyu arc Moho.

6 DISCUSSION

6.1 Mountain building in Taiwan

It has long been debated whether the internal structure of the Taiwan orogen is more consistent with a thick-skinned or thin-skinned
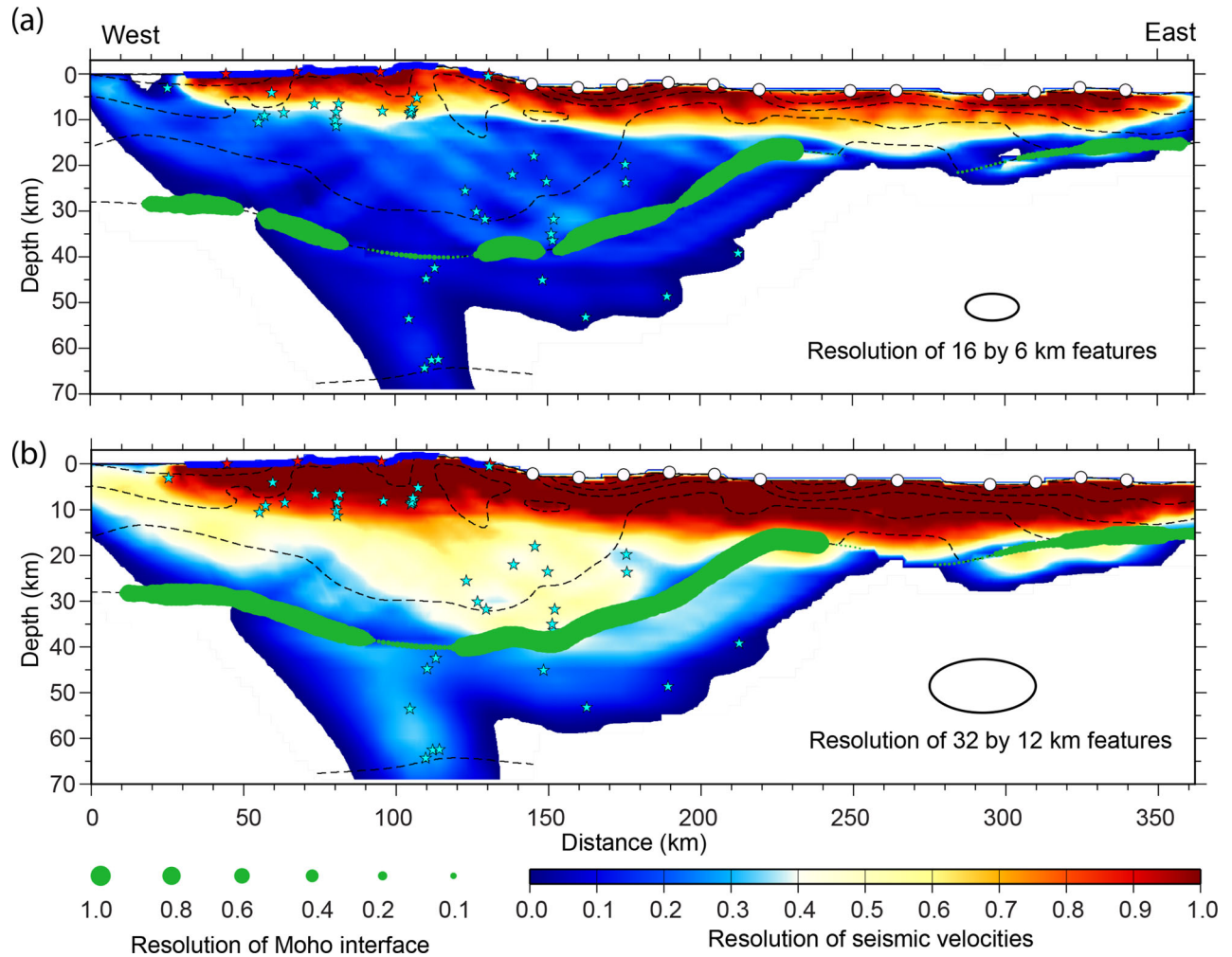
Figure 10. Resolution tests for two different spatial scales, based on the linearized tomographic inversion (Van Avendonk *et al.* 2004). Dashed lines show the seismic velocity contours at 1.0 km s^{-1} intervals; light blue stars mark the earthquakes, white circles the OBSs used in the inversion. The row of dark blue triangles along the surface across Taiwan represent land seismic stations. Red stars mark the location of explosive shots. (a) Resolution of 16 km (horizontal) by 6 km (vertical) ellipse in the T6 seismic velocities, and 16 km section of Moho (solid black). (b) Resolution of a 32 km (horizontal) by 12 km (vertical) ellipse and Moho patch.

tectonic evolution (e.g. Suppe 1981; Wu *et al.* 1997; Brown *et al.* 2012). Our tomographic inversion shows that the seismic velocity structure in the upper crust along our seismic line across northern Taiwan correlates well with the tectonic provinces of the mountain belt. The seismic velocity anomalies associated with the Hsüehshan Range, Lishan Fault and Central Range can be traced to approximately 10–15 km depth (Fig. 9), significantly deeper than the ~10 km deep horizontal band of upper crustal earthquakes in the Taiwan mountain belt (Fig. 9b), which may coincide approximately with the brittle-ductile transition (Kidder *et al.* 2012; Van Avendonk *et al.* 2014). In various local seismotectonic studies of Taiwan, seismicity outlines sub-vertical shear zones that also bound the major tectonic units to approximately the same depth of ~15 km or deeper (Gourley *et al.* 2007; Ching *et al.* 2011a; Brown *et al.* 2012). It is therefore likely that the arc-continent collision deformed the entire crust, and that deformation in the upper and lower crust are coupled.

The northern Hsüehshan Range metasediments derive from an inverted Eocene-Oligocene sedimentary basin that formed on the Eurasian shelf (Clark *et al.* 1993; Tillman & Byrne 1995; Simoes *et al.* 2007). Seismic velocities 5.0–5.5 km s^{-1} in the upper few kilometres are consistent with intermediate, upper greenschist facies

metamorphic basement (Christensen & Mooney 1995). In the adjacent Lishan fault zone, seismic velocities are as low as 4.0 km s^{-1}. Across the Lishan fault to the east, eastern slate belt rocks are Eocene to Miocene in age, and of prehnite-pumpellyite facies (Lee *et al.* 1997). Because of the lower metamorphic grade rocks, seismic wave speed of the slate belt rocks could be lower here than in the Hsüehshan Range. The higher seismic velocities in the Central Range (>6.0 km s^{-1}) are therefore more easily explained by shallow pre-Miocene basement. The Tananao schist, which outcrops in the eastern central Range, contains igneous intrusive and ultramafic rocks as well as marbles that are consistent with observed > 6.0 km s^{-1} velocities.

Between 70 and 135 km in our model (Fig. 9) the lower crust of the Taiwan mountain belt forms a broad crustal root with seismic velocities as low as 6.0 km s^{-1} to a depth of 30 km, and not much higher than 6.5 km s^{-1} at the Moho at 40 km depth. In comparison, the structure of the crustal root along transect T5 (Van Avendonk *et al.* 2014) is quite similar to 30 km depth. Possibly, the lower crust along transect T5 has a deeper root (50 km) with seismic velocities exceeding 7.0 km s^{-1}. Unfortunately, the lower crust and Moho along transect T5 is not as well constrained as along T6,

because no Moho reflections were used to obtain the seismic velocity model for T5. Nonetheless, it is possible that the dense lower crust in central to northern Taiwan delaminated, which would also explain why the orogenic crust is thinner on transect T6 than to the south.

6.2 Ryukyu arc crust

The southern Ryukyu arc platform is a ribbon of continental crust that rifted from the Eurasian margin around 2 Ma, when backarc extension formed the Okinawa Trough (Sibuet *et al.* 1998). Before the backarc opening, this section of the Eurasian margin may have collided with the northernmost section of the Luzon arc, and the continental crust may have thickened in the same manner as we observe in Taiwan at present. During the westward propagation of extension from the Okinawa trough into the Ilan Plain of northeastern Taiwan (Huang *et al.* 2012), the Ryukyu arc basement rotated clockwise by approximately 90° from a NNE to an ESE trend. The degree to which the Ryukyu arc crust offshore Taiwan was deformed in the aftermath of the collision is not well known.

The crust of the Central Range and Ryukyu arc both reach a maximum thickness of 38–40 km near the coast of northeastern Taiwan in our seismic velocity profile, which is good evidence that the collision between the Luzon arc and the Eurasian margin affected the southwestern Ryukyu arc as well. Beneath the mostly undeformed sediments of the Hoping Basin lie tilted strata of the older Suao basin (Lallemand *et al.* 1997) that record deformation of the basement in the adjacent arc-continent collision. The crust of the Ryukyu arc beneath the Hoping Basin has seismic velocities between 5.5 and 6.5 km s^{-1}. This is somewhat higher than in the adjacent Taiwan orogen, where the seismic velocity of the upper and middle crust only exceeds 6.0 km s^{-1} in the eastern Central Range (Fig. 9). High-grade metamorphic rocks may therefore make up a larger proportion of the Ryukyu arc crust (Fabbri & Fournier 1999) than in the Taiwan mountain belt.

The NW-SE oriented TAIGER transect T6 lies obliquely across the Ryukyu arc platform, so we expect that variations in seismic structure can in part be attributed to the general differences between the arc, forearc, and accretionary prism. For example, the Ryukyu crust decreases in thickness from ∼38 km near the Taiwan coast (135 km) to ∼9 km beneath the Nanao Basin (230 km) in our model. Farther east, the base of the Ryukyu crust is not well resolved in our tomographic inversion. In our interpretation of the TAIGER MCS (Fig. 3) and wide-angle seismic data (Fig. 9b) the Ryukyu arc and forearc crust is relatively constant in thickness (9–10 km) beneath the East Nanao Basin to 320 km. Uplift and brittle deformation of the Ryukyu forearc basement between the Nanao and East Nanao basins (Fig. 3) marks the subduction of the north–south trending Gagua Ridge (Lallemand *et al.* 1999). Farther south, this ridge of thickened Philippine Sea Plate ocean crust has been imaged with TAIGER marine seismic refraction data, which supports its interpretation as a Miocene-age failed subduction zone (Eakin *et al.* 2015).

The lateral decrease in seismic velocity in the crust between 300 and 320 km in our seismic velocity profile (Fig. 9) may be representative of the structural variation between the forearc basement and the accretionary prism of the Ryukyu subduction system. This structural boundary has been imaged previously along marine seismic refraction profiles that were oriented perpendicular to the trench system (Wang *et al.* 2001; Klingelhoefer *et al.* 2012).

6.3 Philippine Sea Plate

The north–south structural continuity of the Taiwan mountain belt (Ho 1986) is strong evidence that the Luzon arc collided with northern Taiwan in the early history of the orogen, but it is not clear what happened to the Luzon arc block and northeast corner of the Philippine Sea Plate in the later stages of the collision. The presence of arc volcanic rocks in the Coastal Range (Barrier & Angelier 1986) suggests that the Luzon arc is truly accreted to the Eurasian margin. However, the deep seismic velocity structure along TAIGER transect T5 shows that much of the Luzon arc block may have been pushed to mid-crustal depths in central Taiwan (Van Avendonk *et al.* 2014). Farther north, the Coastal Range terminates south of the intersection with the Ryukyu trench, which may be explained by northward subduction of the Luzon arc along with the Philippine Sea Plate (Wu *et al.* 2009).

In the active-source seismic data from TAIGER transect T6 we did not find direct evidence for the existence of Philippine Sea Plate crust, such as a deep seismic reflection from its top of basement or from its Moho. On the other hand, the earthquake and onshore-offshore arrivals in our data set require ∼7.0 km s^{-1} velocities beneath the base of Eurasian crust east of Taiwan (Fig. 9), which is constrained by *P1P* reflections from the onshore-offshore data (Fig. 8c). This 7.0 km s^{-1} velocity layer is estimated to be just 6 km thick because earthquake and long-offset P2 arrivals in the onshore-offshore data (Fig. 8c) travel with a seismic wave speed of approximately 8.0 km s^{-1}. With the guidance from published seismic velocity models from north-south marine seismic refraction lines across the Ryukyu subduction system (Wang *et al.* 2001; Klingelhoefer *et al.* 2012), we can reconstruct the location of Philippine Sea Plate crust from the strike-slip zone along the coast of northeastern Taiwan to the Ryukyu accretionary wedge (Fig. 9b). Our seismic velocity model does not have sufficient resolution (Fig. 10) to infer whether the subducting Philippine Sea Plate crust is still attached to the Luzon arc along transect T6, but the arc/forearc block could still reside near the east coast of Taiwan at ∼35 km depth.

6.4 Extension of the orogen

The deep mantle seismic velocity structure and the seismicity in Taiwan (Kuo-Chen *et al.* 2012a,b; Huang *et al.* 2014) shows that plate convergence changes in Taiwan from eastward subduction of the Eurasian Plate along transect T5 (Fig. 11d) to northwestward subduction of the Philippine Sea Plate along transect T6 (Fig. 11c). After this change in subduction polarity at ∼2 Ma, rapid roll-back of the Philippine Sea Plate in the Ryukyu subduction zone (Huang *et al.* 2012) appears to have been the leading cause of extensional collapse in the northern Taiwan mountain belt, starting in the Okinawa Trough (Fig. 11b). Topographic stresses (Teng 1996) and orogen-parallel extrusion (Angelier *et al.* 2009) also contributed to the relaxation of the thickened crust. However, the northward subduction of the Luzon arc, which we may now have imaged along transect T6 offshore northeastern Taiwan (Figs 9 and 11c), has removed the backstop that confined the mountain belt. Ryukyu subduction zone backarc extension has since then formed the Ilan Plain (Fig. 2a), a triangular basin that wedges between the Hsüehshan Range and the Central Range (Clift *et al.* 2008). The northern Taiwan mountain belt is subsiding as well, but the rate here is much more modest than in the Ilan Plain (Ching *et al.* 2011b).

While the extension in the upper crust is localized in the Ilan Plain, the lower crustal root reaches its maximum thickness of 40 km beneath it (Fig. 11c). The crust of the Taiwan mountain belt is still
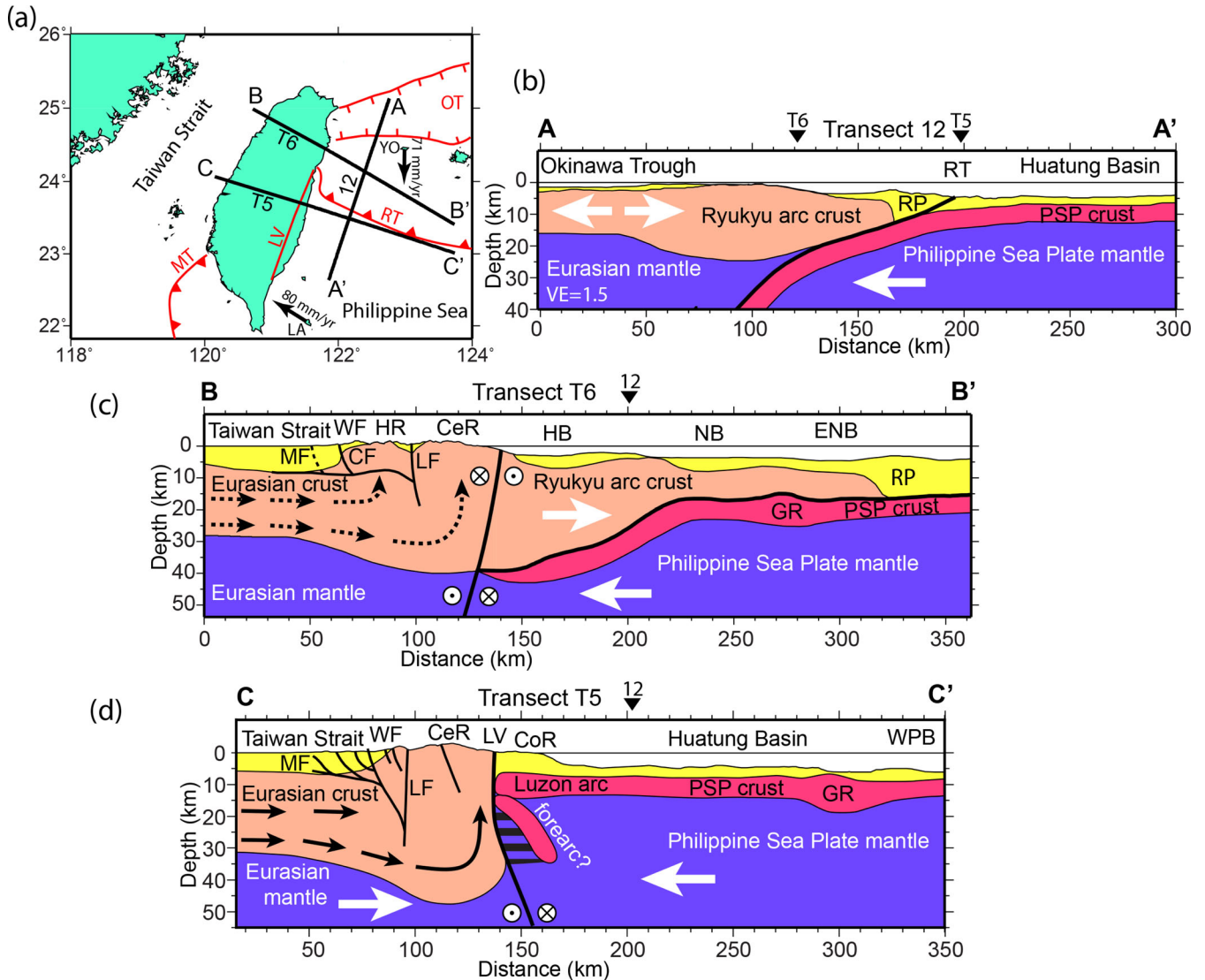
Figure 11. (a) Map showing TAIGER transect 12, T5 and T6, relative to the Manila Trench (MT), Longitudinal Valley (LV), Ryukyu Trench (RT) and Okinawa Trench). The GPS motion vectors of the islands of Yonaguni (YO) (Nakamura 2004) and Lanhsu (LA) (Hsu *et al.* 2009) illustrate plate motions relative to Eurasia. (b) The geometry of the Ryukyu arc and Philippine Sea Plate (PSP) crust, inferred from seismic velocities along TAIGER line 12 (Klingelhoefer *et al.* 2012). White arrows indicate the plate motions projected on this profile. RP, Ryukyu prism; RT, Ryukyu Trench. (c) Tectonic interpretation of the seismic velocity structure along transect T6 (Fig. 9). Dashed black lines indicate the approximate past trajectories of incoming Eurasian crustal rock in the ceased arc-continent collision of northern Taiwan. The white arrow indicates in-line plate motion; the white circles show the out-of-plane motion between the Eurasian and Philippine Sea plates. CF, Chüchih Fault; GR, Gagua Ridge; MF, mountain front. Other abbreviations as in Fig. 9. (d) Interpretation of seismic velocity model of transect T5 (Van Avendonk *et al.* 2014). Solid black lines indicate the approximate past trajectories of incoming Eurasian crustal rock in the ongoing arc-continent collision of central Taiwan. Striped area marks the serpentinized and deformed PSP mantle wedge corner (Van Avendonk *et al.* 2014). CoR, Coastal Range; WPB, West Philippine Basin.

thicker to the south. For example, Van Avendonk *et al.* (2014) found a crustal root to 50 km depth along TAIGER transect T5 in central Taiwan (Fig. 11d). Given the overall difference in crustal thickness between transects T5 and T6, it is quite plausible that the entire crust of the northern Taiwan mountain belt stretched and thinned in the aftermath of arc-continent collision. On the other hand, the arc-continent collision may also have progressed less far in the north, since the subduction of the Coastal Range and the Philippine Sea Plate in northern Taiwan removed the backstop for the Taiwan orogen (Wu *et al.* 2009). Either way, extensional deformation in the lower crust was not localized beneath the Ilan Plain of northeastern Taiwan, and it was more likely distributed over the width of the

mountain belt. The high heat flow in the Taiwan orogen (Lin 2000) implies that the lower crust is relatively hot. It is therefore possible that the crustal root widened and flattened in northern Taiwan (Rey *et al.* 2001), without significant post-collisional deformation of the stronger upper crust of the Taiwan mountain belt west of the Ilan Plain.

7 CONCLUSIONS

From the analysis of wide-angle and local earthquake traveltimes along transect T6 in northern Taiwan we constructed a seismic

velocity model that shows the lithospheric structure of the Taiwan mountain belt and the adjacent Ryukyu arc in unprecedented detail. We summarize the following conclusions:

(1) By combining traveltime data from seismic records of the 2008 and 2009 TAIGER active-source experiments with local earthquakes that were registered by the same instrument arrays, we were able to produce a detailed seismic velocity image of the crustal structure across northern Taiwan. The results from TAIGER transects T5 and T6 illustrate the importance of earthquake traveltimes in tomographic studies of mountain belts with deep crustal roots.

(2) Arc-continent collision in northern Taiwan led to thickening of the Eurasian crust from ∼24 km in the Taiwan Strait to ∼40 km beneath the eastern Central Range. The Luzon arc block and ocean crust and mantle lithosphere of the Philippine Sea Plate that were engaged in this collision have since then subducted northward into the Ryukyu trench system. Our seismic refraction data provide evidence for a remnant of the Philippine Sea Plate crust beneath the Eurasian crust offshore northeastern Taiwan.

(3) Seismic velocity anomalies associated with the Hsüehshan Range, Lishan Fault and Central Range show that these major elements of the Taiwan mountain belt are continue to at least 15 km depth. Our result suggests that rocks exhumed in the Hsüehshan Range and Central Range are exhumed from middle or perhaps lower crustal levels in a near-vertical path.

(4) Though post-orogenic collapse and extension of the upper continental crust along transect T6 is concentrated in the Ilan Plain of northeastern Taiwan, the orogen still has a 40 km deep lower crustal root in this area. Extension of the mountain belt in northern Taiwan was therefore likely accommodated by ductile, distributed deformation.

ACKNOWLEDGEMENTS

REFERENCES

Abers, G.A. & Roecker, S.W., 1991. Deep structure of an arc-continent collision: earthquake relocation and inversion for upper mantle *P* and *S* wave velocities beneath Papua New Guinea, *J. geophys. Res.,* **96,** 6379–6401.

Angelier, J. *et al.,* 2009. Does extrusion occur at both tips of the Taiwan collision belt? Insights from active deformation studies in the Ilan Plain and Pingtung Plain regions, *Tectonophysics,* **466,** 356–376.

Audley-Charles, M., 2004. Ocean trench blocked and obliterated by Banda forearc collision with Australian proximal continental slope, *Tectonophysics,* **389,** 65–79.

Avé Lallemant, H.G., 1997. Transpression, displacement partitioning, and exhumation in the eastern Caribbean/South American plate boundary zone, *Tectonics,* **16,** 272–289.

Barrier, E. & Angelier, J., 1986. Active collision in eastern Taiwan: the Coastal Range, *Tectonophysics,* **125,** 39–72.

Bertrand, E.A. *et al.,* 2009. Magnetotelluric evidence for thick skinned tectonics in Central Taiwan, *Geology,* **37,** 711–714.

Bertrand, E.A. *et al.,* 2012. Magnetotelluric imaging beneath the Taiwan orogen: an arc-continent collision, *J. geophys. Res.,* **117,** B01402, doi:10.1029/2011jb008688.

Bowin, C., Purdy, G.M., Johnston, C., Shor, G., Lawver, L., Hartono, H.M.S. & Jezek, P., 1980. Arc-continent collision in Banda Sea region, *Am. Assoc. Petrol. Geol. Bull.,* **64,** 868–915.

Brown, D. *et al.,* 2011. Arc-continent collision: the making of an orogen, in *Arc-Continent Collision, Frontiers in Earth Sciences,* pp. 477–493, eds Brown, D. & Ryan, P.D., Springer-Verlag.

Brown, D., Alvarez-Marron, J., Schimmel, M., Wu, Y.-M. & Camanni, G., 2012. The structure and kinematics of the central Taiwan mountain belt derived from geological and seismicity data, *Tectonics,* **31,** TC5013, doi:10.1029/2012TC003156.

Byrne, T., Chan, Y.-C., Rau, R.-J., Lu, C.Y., Lee, Y.H. & Wang, Y.J., 2011. The arc-continent collision in Taiwan, in *Arc-Continent-Collision, Frontiers in Earth Sciences,* pp. 213–245, eds Brown, D. & Ryan, P.D., Springer-Verlag.

Camanni, G. *et al.,* 2014. Basin inversion in central Taiwan and its importance for seismic hazard, *Geology,* **42,** 147–150.

Ching, K.-E., Johnson, K.M., Rau, R.-J., Chuang, R.Y., Kuo, L.-C. & Leu, P.-L., 2011a. Inferred fault geometry and slip distribution of the 2010 Jiashian, Taiwan, earthquake is consistent with a thick-skinned deformation model, *Earth planet. Sci. Lett.,* **301,** 78–86.

Ching, K.E., Rau, R.J., Johnson, K.M., Lee, J.C. & Hu, J.C., 2011b. Present-day kinematics of active mountain building in Taiwan from GPS observations during 1995–2005, *J. geophys. Res.,* **116,** B09405, doi:10.1029/2010jb008058.

Chou, Y.-W. & Yu, H.-S., 2002. Structural expressions of flexural extension in the arc-continent collisional foredeep of western Taiwan, in *Geology and Geophysics of an Arc-Continent Collision,* Taiwan, pp. 1–12, eds Byrne, T.B. & Liu, C.-S., Geol. Soc. Am. Spec. Pap. 358.

Christensen, N.I. & Mooney, W.D., 1995. Seismic velocity structure and composition of the continental crust: a global view, *J. geophys. Res.,* **100,** 9761–9788.

Clark, M.B., Fisher, D.M., Lu, C.Y. & Chen, C.H., 1993. Kinematic analyses of the Hsüehshan Range, Taiwan: a large-scale pop-up structure, *Tectonics,* **12,** 205–217.

Clift, P.D., Lin, A.T.S., Wu, F., Draut, A.E., Lai, T.-H., Fei, L.-Y., Schouten, H. & Teng, L., 2008. Post-collisional collapse in the wake of migrating arc-continent collision in the Ilan Basin, Taiwan, in *Formation and Applications of the Sedimentary Record in Arc Collision Zones,* pp. 257–278, eds Draut, A.E., Clift, P.D. & Scholl, D.W., Geol. Soc. Am. Spec. Pap. 436.

Cooper, P. & Taylor, B., 1987. Seismotectonics of New Guinea: a model for arc reversal following arc-continent collision, *Tectonics,* **6,** 53–67.

Dewey, J.F., 1988. Extensional collapse of orogens, *Tectonics,* **7,** 1123–1139.

Draut, A.E. & Clift, P.D., 2013. Differential preservation in the geologic record of intraoceanic arc sedimentary and tectonic processes, *Earth Sci. Rev.,* **116,** 57–84.

Eakin, D.H., McIntosh, K.D., Van Avendonk, H.J.A., Lavier, L., Lester, R., Liu, C.-S. & Lee, C.-S., 2014. Crustal-scale seismic profiles across the Manila subduction zone: the transition from intraoceanic subduction to incipient collision, *J. geophys. Res.: Solid Earth,* **119,** 1–17.

Eakin, D.H., McIntosh, K.D., Van Avendonk, H.J.A. & Lavier, L., 2015. New geophysical constraints on a failed subduction initiation: the structure and potential evolution of the Gagua Ridge and Huatung Basin, *Geochem. Geophys. Geosyst.,* **16,** 380–400.

Fabbri, O. & Fournier, M., 1999. Extension in the southern Ryukyu Arc (Japan); link with oblique subduction and back arc rifting, *Tectonics,* **18,** 486–497.

Fuller, C.W., Willett, S.D., Fisher, D. & Lu, C.Y., 2006. A thermomechanical wedge model of Taiwan constrained by fission-track thermochronometry, *Tectonophysics,* **425,** 1–24.

Geist, E.L. & Scholl, D.W., 1994. Large-scale deformation related to the collision of the Aleutian Arc with Kamchatka, *Tectonics,* **13,** 538–560.

Gourley, J.R., Byrne, T., Chan, Y.-C., Wu, F. & Rau, R.-J., 2007. Fault geometries illuminated from seismicity in central Taiwan: implications for crustal scale structural boundaries in the northern Central Range, *Tectonophysics,* **445,** 168–185.

Ho, C.S., 1986. A synthesis of the geologic evolution of Taiwan, *Tectonophysics,* **125,** 1–16.

Hole, J.A., 1992. Nonlinear high-resolution three-dimensional seismic travel time tomography, *J. geophys. Res.,* **97,** 6553–6562.

Hou, C.-S. *et al.*, 2009. The crustal deformation of the Ilan Plain acted as a westernmost extension of the Okinawa Trough, *Tectonophysics,* **466,** 344–355.

Huang, C.Y., Yuan, P.B. & Tsao, S.J., 2006. Temporal and spatial records of active arc-continent collision in Taiwan: a synthesis, *Bull. geol. Soc. Am.,* **118,** 274–288.

Huang, H.-H., Shyu, J.B.H., Wu, Y.-M., Chang, C.-H. & Chen, Y.-G., 2012. Seismotectonics of northeastern Taiwan: kinematics of the transition from waning collision to subduction and postcollisional extension, *J. geophys. Res.,* **117,** B01313, doi:10.1029/2011JB008852.

Huang, H.-H., Wu, Y.-M., Song, X., Chang, C.-H., Lee, S.-J., Chang, T.-M. & Hsieh, H.-H., 2014. Joint Vp and Vs tomography of Taiwan: implications for subduction-collision orogeny, *Earth planet. Sci. Lett.,* **392,** 177–191.

Huang, W.J., Johnson, K.M., Fukuda, J. & Yu, S.B., 2010. Insights into active tectonics of eastern Taiwan from analyses of geodetic and geologic data, *J. geophys. Res.,* **115,** B03413, doi:10.1029/2008JB006208.

Hsu, Y., Yu, S., Simons, M., Kuo, L. & Chen, H., 2009. Interseismic crustal deformation in the Taiwan plate boundary zone revealed by GPS observations, seismicity, and earthquake focal mechanisms, *Tectonophysics,* **479,** 4–18.

Kidder, S., Avouac, J.-P. & Chan, Y.-C., 2012. Constraints from rocks in the Taiwan orogen on crustal stress levels and rheology, *J. geophys. Res.,* **117,** B09408, doi:10.1029/2012JB009303.

Kim, K.-H., Chiu, J.-M., Kao, H., Liu, Q. & Yeh, Y.-H., 2004. A preliminary study of crustal structure in Taiwan region using receiver function analysis, *Geophys. J. Int.,* **159,** 146–164.

Klingelhoefer, F., Berthet, T., Lallemand, S., Schnurle, P., Lee, C.-S., Liu, C.-S., McIntosh, K. & Theunissen, T., 2012. *P*-wave velocity structure of the southern Ryukyu margin east of Taiwan: results from the ACTS wide-angle seismic experiment, *Tectonophysics,* **578,** 50–62.

Konstantinovskaya, E., 2011. Early Eocene arc-continent collision in Kamchatka, Russia: structural evolution and geodynamic model, in *Arc-Continent Collision, Frontiers in Earth Sciences,* pp. 247–277, eds Brown, D. & Ryan, P.D., Springer Verlag.

Kroehler, M.E., Mann, P., Escalona, A. & Christeson, G.L., 2011. Late Cretaceous-Miocene diachronous onset of back thrusting along the South Caribbean deformed belt and its importance for understanding processes of arc collision and crustal growth, *Tectonics,* **30,** Tc6003, doi:10.1029/2011tc002918.

Kuo-Chen, H., Wu, F.T. & Roecker, S.W., 2012a. Three-dimensional P velocity structures of the lithosphere beneath Taiwan from the analysis of TAIGER and related seismic data sets, *J. geophys. Res.,* **117,** B06306, doi:10.1029/2011jb009108.

Kuo-Chen, H., Wu, F.T., Jenkins, D.M., Mechie, J., Roecker, S.W., Wang, C.Y. & Huang, B.S., 2012b. Seismic evidence for the α-β quartz transition beneath Taiwan from Vp/Vs tomography, *Geophys. Res. Lett.,* **39,** L22302, doi:10.1029/2012GL053649.

Lacombe, O., Mouthereau, F., Angelier, J., Chu, H.-T. & Lee, J.-C., 2003. Frontal belt curvature and oblique ramp development at an obliquely collided irregular margin: Geometry and kinematics of the NW Taiwan fold-thrust belt, *Tectonics,* **22,** 1025, doi:10.1029/TC001436.

Lallemand, S., Liu, C.S. & Font, Y., 1997. A tear fault boundary between the Taiwan orogen and the Ryukyu subduction zone, *Tectonophysics,* **274,** 171–190.

Lallemand, S., Liu, C.S., Dominguez, S., Schnurle, P., Malavieille, J. & Scientific Crew, ACT., 1999. Trench-parallel stretching and folding of forearc basins and lateral migration of the accretionary wedge in the southern Ryukyus: a case of strain partition caused by oblique convergence, *Tectonics,* **18,** 231–247.

Lallemand, S., Theunissen, T., Schnürle, P., Lee, C.-S., Liu, C.-S. & Font, Y., 2013. Indentation of the Philippine Sea plate by the Eurasia plate in Taiwan: details from recent marine seismological experiments, *Tectonophysics,* **594,** 60–79.

Lee, J.C., Angelier, J. & Chu, H.T., 1997. Polyphase history and kinematics of a complex major fault zone in the northern mountain belt: the Lishan fault, *Tectonophysics,* **274,** 97–115.

Lee, Y.H., Chen, C.C., Liu, T.K., Ho, H.C., Lu, H.Y. & Lo, W., 2006. Mountain building mechanisms in the Southern Central Range of the Taiwan Orogenic Belt—from accretionary wedge deformation to arc-continental collision, *Earth planet. Sci. Lett.,* **252,** 413–422.

Lester, R. & McIntosh, K., 2012. Multiple attenuation in crustal-scale imaging: examples from the TAIGER marine reflection data set, *Mar. geophys. Res.,* **33,** 289–305.

Lester, R., McIntosh, K., Van Avendonk, H.J.A., Lavier, L., Liu, C.-S. & Wang, T.K., 2013. Crustal accretion in the Manila trench accretionary wedge at the transition from subduction to mountain-building in Taiwan, *Earth planet. Sci. Lett.,* **375,** 430–440.

Lin, C.-H., 2000. Thermal modeling of continental subduction and exhumation constrained by heat flow and seismicity in Taiwan, *Tectonophysics,* **324,** 189–201.

Lin, A.T., Watts, A.B. & Hesselbo, S.P., 2003. Cenozoic stratigraphy and subsidence history of the South China Sea margin in the Taiwan region, *Basin Res.,* **15,** 453–478.

Liu, T.K., Hsieh, S., Chen, Y.G. & Chen, W.S., 2001. Thermo-kinematic evolution of the Taiwan oblique-collision mountain belt as revealed by zircon fission track dating, *Earth planet. Sci. Lett.,* **186,** 45–56.

McIntosh, K., Nakamura, Y., Wang, T.-K., Shih, R.-C., Chen, A. & Liu, C.-S., 2005. Crustal-scale seismic profiles across Taiwan and the western Philippine Sea, *Tectonophysics,* **401,** 23–54.

McIntosh, K., Van Avendonk, H., Lavier, L., Lester, W.R., Eakin, D., Wu, F., Liu, C.-S. & Lee, C.-S., 2013. Inversion of a hyper-extended rifted margin in the southern Central Range of Taiwan, *Geology,* **41,** 871–874.

Moser, T.J., 1991. Shortest path calculation of seismic rays, *Geophysics,* **56,** 59–67.

Moser, T.J., Nolet, G. & Snieder, R.K., 1992. Ray bending revisited, *Bull. seism. Soc. Am.,* **82,** 259–288.

Mouthereau, F. & Lacombe, O., 2006. Inversion of the Paleogene Chinese continental margin and thick-skinned deformation in the Western Foreland of Taiwan, *J. Struct. Geol.,* **28,** 1977–1993.

Nakamura, M., 2004. Crustal deformation in the central and southern Ryukyu Arc estimated from GPS data, *Earth planet. Sci. Lett.,* **217,** 389–398.

Rey, P., Vanderhaeghe, O. & Teyssier, C., 2001. Gravitational collapse of the continental crust: definition, regimes and modes, *Tectonophysics,* **342,** 435–449.

Sibuet, J.-C., Deffontaines, B., Hsu, S.-K., Thareau, N., Le Formal, J.-P, Liu, C.-S. & ACT party, 1998. Okinawa trough backarc basin: early tectonic and magmatic evolution, *J. geophys. Res.,* **103,** 30 245–30 267.

Simoes, M. & Avouac, J.P., 2006. Investigating the kinematics of mountain building in Taiwan from the spatiotemporal evolution of the foreland basin and western foothills, *J. geophys. Res.,* **111,** B10401, doi:10.1029/2005JB004209.

Simoes, M., Avouac, J.P., Beyssac, O., Goffe, B., Farley, K.A. & Chen, Y.G., 2007. Mountain building in Taiwan: a thermokinematic model, *J. geophys. Res.,* **112,** B11405, doi:10.1029/2006jb004824.

Teng, L.S., 1990. Geotectonic evolution of late Cenozoic arc—continent collision in Taiwan, *Tectonophysics,* **183,** 57–76.

Teng, L.S., 1996. Extensional collapse of the northern Taiwan mountain belt, *Geology,* **24,** 949–952.

Suppe, J., 1981. Mechanics of mountain building and metamorphism in Taiwan, *Mem. geol. Soc. China,* **4,** 67–89.

Suppe, J., 1984. Kinematics of arc-continent collision, flipping of subduction, and backarc spreading near Taiwan, *Mem. geol. Soc. China,* **6,** 21–33.

Theunissen, T., Lallemand, S., Font, Y., Gautier, S., Lee, C.-S., Liang, W.-T., Wu, F. & Berthet, T., 2012. Crustal deformation at the southernmost part of the Ryukyu subduction (East Taiwan) as revealed by new marine seismic experiments, *Tectonophysics,* **578,** 10–30.

Tillman, K.S. & Byrne, T.B., 1995. Kinematic analysis of the Taiwan Slate Belt, *Tectonics,* **14,** 322–341.

Toomey, D.R., Solomon, S.C. & Purdy, G.M., 1994. Tomographic imaging of the shallow crustal structure at 9°30′N, *J. geophys. Res.,* **99,** 24 135–24 157.

Van Avendonk, H.J.A., Harding, A.J., Orcutt, J.A. & Holbrook, W.S., 2001. Hybrid shortest path and ray bending method for traveltime and raypath calculations, *Geophysics,* **66,** 648–653.

Van Avendonk, H.J.A., Shillington, D.J., Holbrook, W.S. & Hornbach, M.J., 2004. Inferring crustal structure in the Aleutian arc from a sparse wide-angle seismic data set, *Geochem. Geophys. Geosyst.,* **5,** Q08008, doi:10.1029/2003GC000664.

Van Avendonk, H.J.A. *et al.*, 2014. Deep crustal structure of an arc-continent collision: constraints from seismic travel times in central Taiwan and the Philippine Sea, *J. geophys. Res.: Solid Earth,* **119,** 8397–8416.

Wang, T.K., McIntosh, K., Nakamura, Y., Liu, C.-S. & Chen, H.-W., 2001. Velocity-interface structure of the southwestern Ryukyu subduction zone from EW9509-1 OBS/MCS data, *Mar. geophys. Res.,* **22,** 265–287.

Wessel, P., Smith, W.H.F., Scharroo, R., Luis, J.F. & Wobbe, F., 2013. Generic Mapping Tools: improved version released, *EOS, Trans. Am. geophys. Un.,* **94,** 409–410.

Willett, S.D. & Brandon, M.T., 2002. On steady states in mountain belts, *Geology,* **30,** 175–178.

Wu, F.T., Rau, R.J. & Salzberg, D., 1997. Taiwan orogeny: thin-skinned or lithospheric collision?, *Tectonophysics,* **274,** 191–220.

Wu, F.T., Liang, W.-T., Lee, J.-C., Benz, H. & Villasenor, A., 2009. A model for the termination of the Ryukyu subduction zone against Taiwan: a junction of collision, subduction/separation, and subduction boundaries, *J. geophys. Res.,* **114,** B07404, doi:10.1029/2008JB005950.

Wu, F.T., Kuo-Chen, H. & McIntosh, K.D., 2014. Subsurface imaging, TAIGER experiments and tectonic models of Taiwan, *J. Asian Earth Sci.,* **90,** 173–208.

Yu, S.-B. & Kuo, L.-C., 2001. Present-day crustal motion along the Longitudinal Valley Fault, eastern Taiwan, *Tectonophysics,* **333,** 199–217.

Yue, L.-F., Suppe, J. & Hung, J.-H., 2005. Structural geology of a classic thrust belt earthquake: the 1999 Chi-Chi earthquake Taiwan (Mw∼7.6), *J. Struct. Geol.,* **27,** 2058–2083.